Acta Technica *62* No. 2B/2017, 105–116

The analysis and application of B-H curves shearing in adjustable inductors[1]

Zhengrong Jiang[2], Jingjiang Qu[2], Jiahui Li[2]

Abstract. The desirable characteristics of the orthogonal inductor are explained by the mathematical and experimental analysis, and those important characteristics are derived from an inclining $B-H$ curve. The effective constitution of the grain oriented lamination core presented here is capable of representing the response of the core subject to the orthogonal magnetization. Considering the DC bias field as an additional anisotropy and magnetostrictive energy, the effective constitutive is satisfactory for describing the effect on hysteresis loop caused by the DC orthogonal bias current. Thus it is anticipated that the method will provide a helpful base for the designing of such kind of inductor. The conclusion can be summarized as the following: The orthogonal bias field can be regarded as an extra energy, which changes the magnetization characteristics of the core of inductor. The inclining B-H plane is created with various DC bias currents put on the inductor, and when the working point is in the linear region of the plane, the linearity of the control characteristics can be gained. The characteristic of the orthogonal inductor is suitable for improving the performance of the passive filter, and the harmonic content can be decreased remarkably with the application of the orthogonal technology. Due to the arrangement of the AC winding and DC bias winding, the decoupling effect is significant. The advantage is beneficial for the application in EVH and UVH transmission system.

Key words. Adjustable inductor, $B-H$ curve, magnetization, harmonic, simulation.

1. Introduction

An adjustable inductor based on orthogonal magnetization shows that it offers some desirable advantages, such as linear regulation, and higher safety in the application of EVH or UVH and lower loss. Most of advantages are derived from the special magnetization mechanism, which must be analyzed, taking into account the movement of domains. A magnetization relation of DC exciting field and AC ex-

[1]This work was sponsored by National Natural Science Foundation of China (51377006) and Beijing Natural Science Foundation (3132008).

[2]School of Electrical and Control Engineering, North China University of Technology, Beijing, 100144, China

citing field has been researched in [1]. In [2],the extra energy is used to analyze the magnetizing process and deduce the mathematical formulas. For the analysis of the DC bias field, the finite element method is applied to model the magnetic distribution on the ferrite inductor [3]. Due to the domain moving involved in the orthogonal magnetization, it requires to study the characteristics of $B-H$ curves to figure out how the bias field affects magnetizing process. In the proposed work, the analysis differs from above-mentioned methods, and here the analysis mainly considers tensor permeability in the core which is subject to orthogonal fields; it is a special consideration under an orthogonal magnetization [4], so $B-H$ curves under the orthogonal bias field are investigated firstly, and then the hysteresis is modeled by comparing the performance of the magnetic material under the action of compressive stress; finally, a prototype inductor is presented, the characteristics are measured and the filter application is discussed. With the calculation and measurement results, relative conclusions are deducted for the magnetization mechanism and applications.

2. State of the art

The strong correlation between the inductance and reluctance has not only been used to elucidate the magnetic mechanism, the design of magnetic structure and decomposition of all kinds of losses, but it has also been selected to change the inductance, and the specific strategic adjustment of the inductive reactive power often becomes the concept of the electromagnetic table.

As an important component for limiting overvoltage, improving power quality and providing reactive power compensation, reactor plays an important role in the stable operation of power network. The expansion of network capacity makes the system short-circuit capacity ratings increase rapidly. In order to limit the short-circuit current, power transmission line protection device must be installed, reactor, that can reduce the short-circuit current and voltage of the short-circuit while the system remains unchanged. Series reactors are mainly used to limit short circuit currents, while shunt reactors are used to adjust the operating voltage of power lines. Shunt reactors are widely used on long distance AC transmission lines, for absorbing excessive reactive power of light load or no-load lines. In UHV and EHV transmission systems, shunt reactor is of special significance, it can improve the transmission capacity of the power system, reduce over-voltage and so on. In the application of the arc suppression coil, shunt reactor provides an inductive current to counteract the capacitive current when the arc suppression coil is grounded, therefore protecting the power equipment.

However, a fixed reactor has some disadvantages, such as:

(1) A fixed reactor reduce the voltage regulating ability when system characteristic changes.

(2) A fixed reactor bring about the power loss when the transmission system is in heavy load.

(3) A fixed reactor increases the equivalent impedance, weakening the line power transmission capacity. In addition, it becomes an additional burden of the transmis-

sion line under heavy load conditions.

2.1. Methodology

The schematic structure of the orthogonal adjustable inductor is shown in Fig. 1. It contains a cylindrical hollow core made of grain-oriented Fe-Si lamination. The overall size of the core is 120×150×80 mm. The toroidal DC winding with 150 turns goes through the bore of the core; outside of the cylinder core, there is a main coil with 220 turns which is connected with power system and creates the AC exciting field in the axial direction. The toroidal winding, like DC bias winding, is connected with DC power to create bias field in the circumferential direction. The two fields are orthogonal to each other.

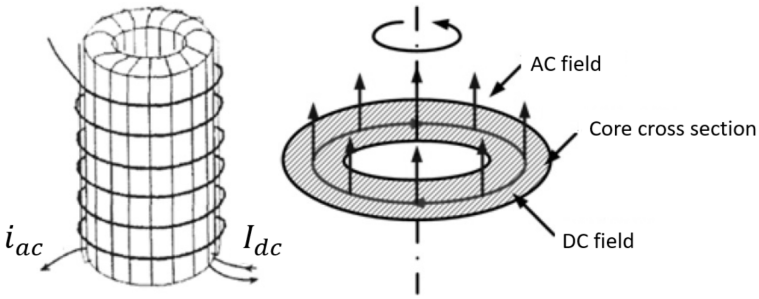

Fig. 1. Configuration of the orthogonal inductor

In order to reduce the effect of demagnetization, two yokes made up of grain-oriented silicon lamination are used, and $B-H$ curves are measured on S&T tester platform. The platform is used to measure the magnetization process of the inductor core under AC field and DC field. It is obvious that $B-H$ curves change with the increase of DC field when the alternating excitation gives $H_{\mathrm{ac}} = 50\,\mathrm{A/m}$ and the $B-H$ curves inclines with the increase of the DC field. Meanwhile, the area of $B-H$ curves decreases simultaneously, which means that the remanence and coercivity descend as well [5].

It appears that $B-H$ curve rotates clockwise in the loci plane remarkably with the increase of the DC bias field. When DC bias current reaches 5 A, the $B-H$ curve becomes a straight line and the enclosed area nearly decreases up to zero, but the magnetization curve has no noticeable hysteresis. However, in case of open path, there is a strong demagnezation field in two terminals [6], even when the AC exciting and DC bias fields have a higher amplitude, and the magnetization process is not completely reversible. In this case, the bias field can be used to adjust the inductance of inductor with this kind of core by altering the effective internal AC field, and the variable range becomes more pronounced due to the shortening of the air path. For the semi-core variable inductor, the inductance is described as

$$L = \frac{\overline{\mu} n^2 D\delta}{l}\,. \tag{1}$$

Here, n is the number of main winding turns, D is the external diameter of the core, δ is the net thickness of the core and l is the core length. Symbol $\overline{\mu}$ is determined by DC bias current while the main current is constant.

Measurement results show that the linearity of the $B-H$ curves is increasing with the increase of the DC bias current. The fact brings about a characteristic of linear permeability. This derives from two facts: one is that the bias winding independent on the ac winding, so there is no mutual inductance between the two windings. The other is that the reversible domain motion is the main process in the initial magnetization, while domain rotation plays a role in the later magnetization [7]. It is contrary to the magnetization in the axial direction. Hence the DC bias field strengthens the reversibility motion ac flux. Due to the demagnetization in the iron core, the effect of the DC bias field on the ac direction is no longer pronounced even if the bias field is higher.

The domain movement is studied toward a perpendicular direction when a press strain works on magnetic material [8]. The effect on hystersis of magnetic material is similar to that of the orthogonal field. So the orthogonal magnetization modeling can be derived referring to the effect caused by the compressive stress.

The magnetization movement in Cartesian coordinates is as shown in Fig. 2.

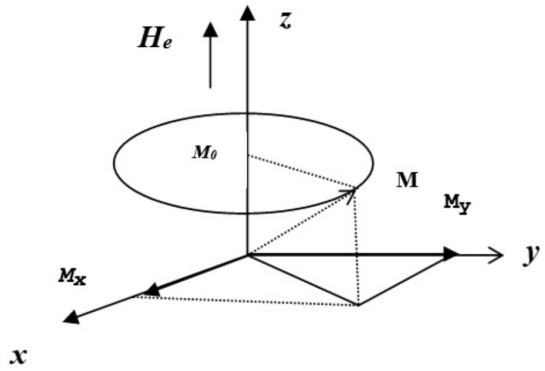

Fig. 2. Magnetization movement in Cartesian coordinates

When the DC bias field increases, an additional anisotropy energy and elastic energy can be effectively calculated and included into the generalized anhysteretic function described previously [9], and the energy E of domains can be described as

$$E = -\mu_0 m \cdot (H_{\parallel} + H_{\perp} + \alpha M) + \widetilde{E}_{\mathrm{an}} + \widetilde{E}_{\sigma}\,. \tag{2}$$

Here, $H_{\parallel}$ means the DC H field whose direction is parallel to AC H field and $H_{\perp}$ means the DC H field whose direction is perpendicular to AC H field.

From the minimum energy theory, the magnetic material will get elastic distortion when the magnetization changes, so the modeling of domain rotating can be established to analyze the changing of the system energy [10]. All these phenomena are connected with the magneto mechanical field, which can be described as follows:

$$E_H = -\mu_0 M_\mathrm{s} H(\cos\theta_1\cos\phi_1 + \cos\theta_2\cos\phi_2 + \cos\theta_3\cos\phi_3)\,, \tag{3}$$

$$\widetilde{E}_\mathrm{an} = E_0 + K_1(\cos^2\theta_1\cos^2\theta_2 + \cos^2\theta_2\cos^2\theta_3 + \cos^2\theta_3\cos^2\theta_1)\,. \tag{4}$$

$$\begin{aligned}\widetilde{E}_\sigma = -\frac{3}{2}\lambda_{100}\sigma(\cos^2\theta_1\cos^2\beta_1 + \cos^2\theta_2\cos^2\beta_2 + \cos^2\theta_3\cos^2\beta_3) + \\ - 3\lambda_{111}\sigma(\cos\theta_1\cos\theta_2\cos\beta_1\cos\beta_2 + \cos\theta_2\cos\theta_3\cos\beta_2\cos\beta_3 + \\ + \cos\theta_3\cos\theta_1\cos\beta_3\cos\beta_1)\,,\end{aligned}$$

$$\overline{\mu_{ij}} = \frac{1}{8\pi^2}\int_0^\pi\int_0^{2\pi}\int_0^{2\pi}\mu_{ij}(\theta,\varphi,\psi)\sin\theta\,\mathrm{d}\psi\,\mathrm{d}\varphi\,\mathrm{d}\theta\,. \tag{5}$$

Here, $\widetilde{E}_\mathrm{an}$ is the effective anisotripic energy, E_H is the exciting field energy, $\widetilde{E}_\sigma$ is the effective magnetostrictive energy, θ_{1--3}, ϕ_{1--3}, β_{1--3} are the mean three directions of the turning magnetic domains in the local coordinate system (indices 1–3 correspond to three conditions) M and H, effective strain force and grain axial direction, respectively. The total energy is

$$E_\mathrm{total} = E_\mathrm{H} + \widetilde{E}_\mathrm{an} + \widetilde{E}_\sigma\,. \tag{6}$$

The effective constitutive equation can be presented as

$$B_i = q_{ijk}\sigma_{kl} + \mu_{ij}H_j + J_i^r\,, \tag{7}$$

where q_{ijk} is the magnetostrictive coefficient, σ_{kl} is the stress tensor, μ_{ij} is the permeability tensor, and J_i^r is the remanent magnetization. Because of the hysteresis of the grain oriented lamination, the direction of M deviates the sum vector of two H fields. Like the analysis mentioned above, the bias field is effective on an additional magnetostrictive energy. In order to explain the magnetization process under the bias field, a perturbation equations is necessary [2].

The anhysteretic function can be quoted as

$$M_\mathrm{aniso} = M_\mathrm{s}\frac{\sum_{\mathrm{all-moments}}\mathrm{e}^{-\frac{E}{k_\mathrm{B}T}}\cos\theta}{\sum_{\mathrm{all-moments}}\mathrm{e}^{-\frac{E}{k_\mathrm{B}T}}}\,. \tag{8}$$

When the orthogonal bias field is increased according to equation (8) (k_B denoting the Boltzmann constant), the change of E makes $B-H$ hysteresis "shearing", which is a quantitative agreement with the experimental result.

The additional anisotropy energy affects the magnetization of the grain-oriented core, which can be calculated from the following equation [11]. The corresponding anhysteresis can be gained and the result curves are shown in Fig. 3.

$$\frac{\mathrm{d}M}{\mathrm{d}H} = (1-c)\frac{M_\mathrm{an}-M}{\delta k - \alpha\,(M_\mathrm{an}-M)} + c\frac{\mathrm{d}M_\mathrm{an}}{\mathrm{d}H}\,. \tag{9}$$

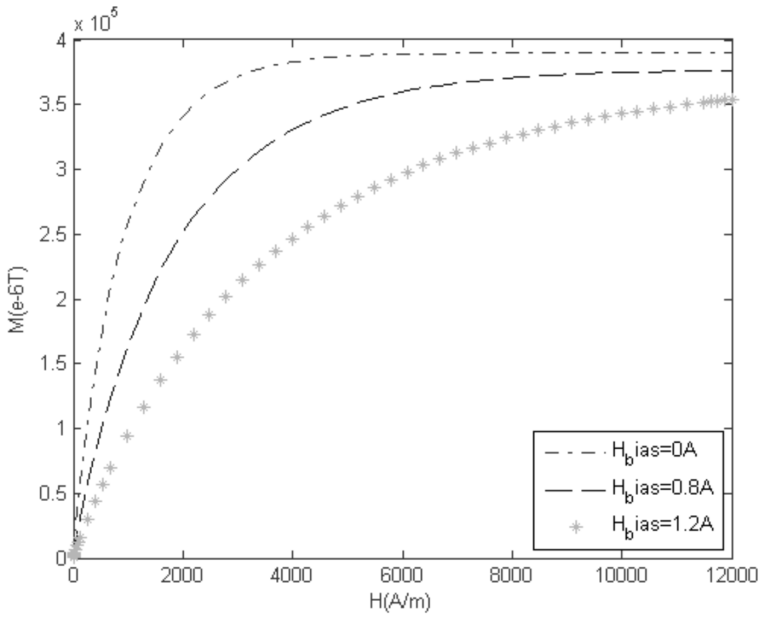

Fig. 3. Anhysteresises under various DC bias currents

3. Result analysis and discussion

Generally, a saturation adjustable inductor is based on the controlled saturation in part of the magnetic circuit, and the permeability and saturation are two of the critical magnetic properties [12]. A constant permeability is nearly a flat magnetization curve across the origin of the $B-H$ plane, and the saturation magnetization at a high field can be described by a horizontal line in the $B-H$ plot, as is shown in Fig. 4. When the DC bias current increases, the magnetization curve will vary gradually from the constant permeability regime to the saturation one. Therefore, the core operating point is critical for the accurate changing of the reactance of the inductor [6].

When the DC bias current increases, a bias flux sums the ac flux in the core and the working point shifts into the non-linear area; the output current becomes distorted due to the non-linearity [13]. For example, when the working point moves from b to a, the output current waveform is changed from 3' to 2'. So the inductance changes with the DC bias flux. With the continuing increase of the DC current, the working point gets closer to the saturate area, and the inductance decreases remarkably. Accordingly, the harmonic content becomes worse.

It is obvious that the non-linearity of the magnetization curve leads to a substantial harmonic distortion. On the contrary, when the operating points are retained in the linear region of $B-H$ "cluster", the output current waveform can be expected to retain sinusoidally in a wide control region, as is shown in Fig. 5. The FEM analysis

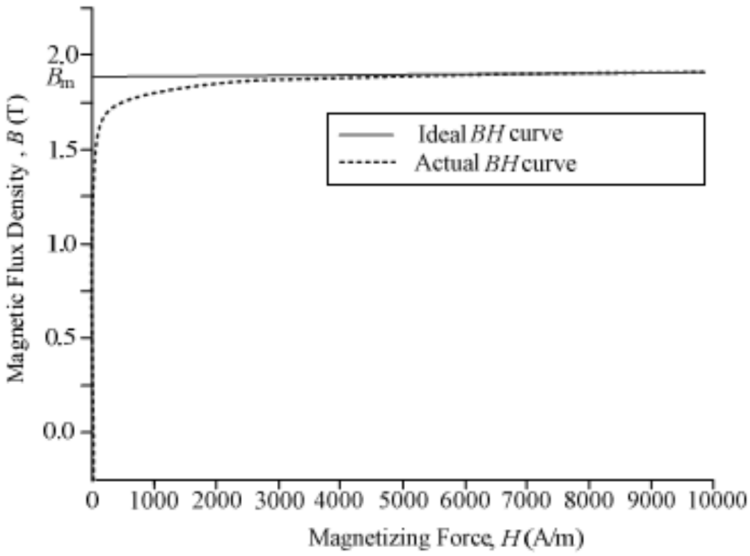

Fig. 4. Ideal and actual $B - H$ curves

also supports the estimation [14].

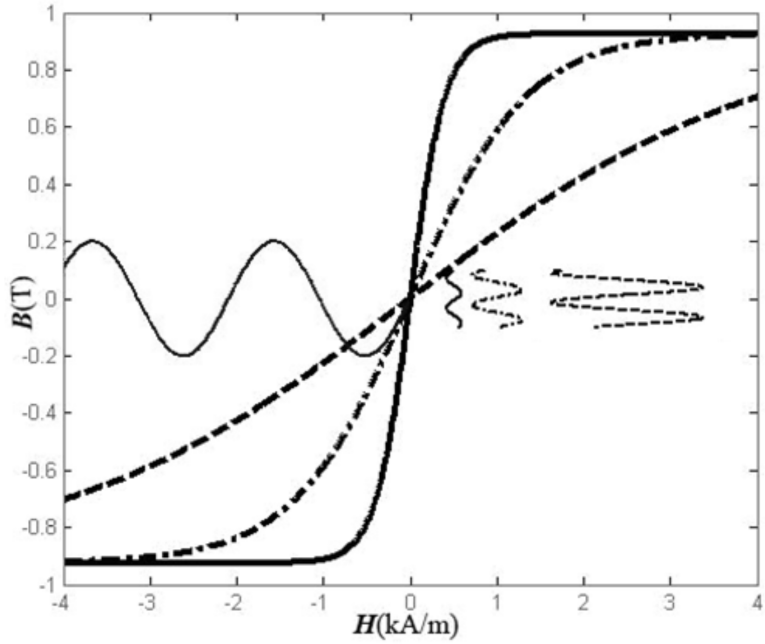

Fig. 5. $B - H$ clusters result in sinusoidal wave

Here, the particular curves represent the typical $B - H$ loops—characteristics of

the magnetic material.

The orthogonal adjustable inductor is expected to achieve the goal mentioned above. In the case of $B-H$ cluster, each curve can be expressed as two lines, and the cluster can be simply described as a lot of lines with differential incline angles, as are shown in Fig. 6.

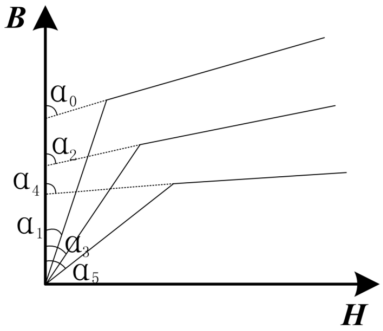

Fig. 6. $B-H$ simple descriptions

Then $B-H$ curve can be described as

$$H = B\tan\alpha_1 \quad \text{for} \quad B < B_{\mathrm{s}}\,,$$

$$H = (B - B_{\mathrm{s}})\tan\alpha_0 \quad \text{for} \quad B > B_{\mathrm{s}}\,. \tag{10}$$

So the working winding current is described as

$$i_{\mathrm{ac}} = (1/2B_{\mathrm{m}}\tan\alpha_0)\bullet$$

$$\begin{gathered}(-B_m\cos\omega t + B_0)\tan\alpha_1 - B_m\cos\omega t + B_0 < B_s \\ (-B_m\cos\omega t + B_0 - B_s)\tan\alpha_1 - B_m\cos\omega t + B_0 > B_s\end{gathered} \tag{11}$$

Using Fourier series analysis, the harmonic current values are gained, as is shown in Fig. 7.

Here the horizontal axis represents the angle between B and H and vertical axis denotes the harmonic content per unit.

It is obvious that the linearity of the permeability is improved with the increase of the orthogonal field , so the harmonic characteristic of the inductor becomes better with the increase of the orthogonal field.

In order to verify the harmonic characteristic of the inductor, an experiment is performed and the experiment circuit is shown in Fig. 8.

Here, U_{e} is AC power which is connected with the working winding of the inductor, U_{s} is the DC power which is connected with DC bias winding, R1 and R2 are changeable resistances, and X1 is the adjustable inductor. Given $U_{\mathrm{e}} = 220\,\mathrm{V}$, through changing DC bias current, based on the experiment results, the harmonic

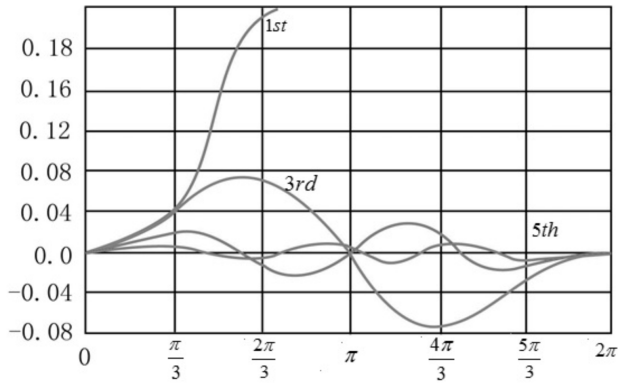

Fig. 7. Incline angles versus harmonics per unit

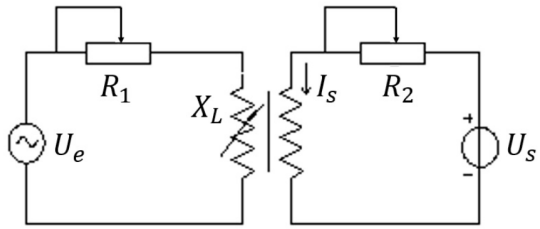

Fig. 8. Experimental platform

characteristic is gained, as is shown in Fig. 9.

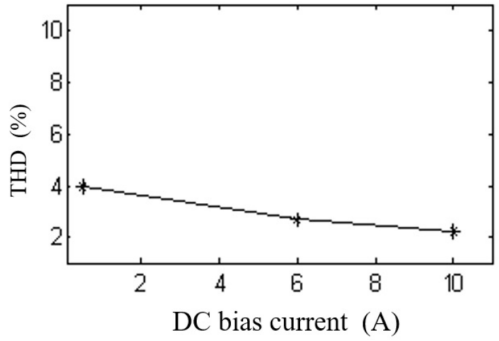

Fig. 9. Harmonic characteristics of the orthogonal magnetization inductor

4. Conclusion

The desirable characteristics of the orthogonal inductor are explained by the mathematical and experimental analysis, and those important characteristics are

derived from an inclining B-H curve. The effective constitution of the grain oriented lamination core presented here is capable of representing the response of the core subject to the orthogonal magnetization. Considering the DC bias field as an additional anisotropy and magnetostrictive energy, the effective constitution is satisfactory for describing the effect on hysteresis loop caused by the DC orthogonal bias current. Thus it is anticipated that the method will provide a helpful base for the designing of such kind of inductor. The conclusion can be summarized as the following: The orthogonal bias field can be regarded as an extra energy, which changes the magnetization characteristics of the core of inductor. The inclining B-H plane is created with various DC bias currents applied to the inductor, and when the working point is in the linear region of the plane, the linearity of the control characteristics can be gained. The characteristic of the orthogonal inductor is suit for improving the performance of the passive filter, and the harmonic content can be reduced remarkably with the application of the orthogonal technology. Due to the arrangement of the AC winding and DC bias winding, the decoupling effect is significant. The advantage is beneficial for the application in EVH and UVH transmission systems.

References

[1] Q. Yu, X. Wang, Y. Cheng: *Electromagnetic modeling and analysis of can effect of a canned induction electrical machine*. IEEE Transactions on Energy Conversion *31* (2016), No. 4, 1471–1478.

[2] D. Hu, J. Sheng, J. Ma, L. Yao,Z. Y. Li, Z. Hong, Z. Jin: *Characteristic tests and electromagnetic analysis of an HTS partial core transformer*. IEEE Transactions on Applied Superconductivity *26* (2016), No. 4, Article No. 5500305.

[3] S. Shen, Y. Tang, L. Ren, Z. Wang: *Electromagnetic calculation of a 35 kV/3.5 MVA single-phase HTS controllable reactor with field–circuit coupled-FEM*. IEEE Transactions on Applied Superconductivity *26* (2016), No. 7, Article No. 5603305.

[4] B. Gustavsen, M. Runde, T. M. Ohnstad: *Wideband modeling, field measurement, and simulation of a 420-kV variable shunt reactor*. IEEE Transactions on Power Delivery *30* (2015), No. 3, 1594–1601.

[5] S. Mukhopadhyay, D. Maiti, A. Banerji, S. K. Biswas, N. K. Deb: *A new harmonic reduced three-phase thyristor-controlled reactor for static VAr compensators*. IEEE Transactions on Industrial Electronics *64* (2017), No. 9, 6898–6907.

[6] M. Young, Z. Li, A. Dimitrovski: *Modeling and simulation of continuously variable series reactor for power system transient analysis*. Proc. IEEE Power and Energy Society General Meeting (PESGM), 17–21 July 2016, Boston, MA, USA, IEEE Conference Publications (2016), 1–5.

[7] Z. Deng, X. Wang, F. Zhou, X. Lei, K. Yu, Y. Qiu: *Modeling of extra-high voltage magnetically controlled shunt reactor*. Proceedings of the CSEE *28* (2008), No. 36, 108–113.

[8] S. S. Sinha, J. Shah, H. Nerkar: *Harmonics measurement using FFT algorithm in digital signal controller for smart micro-grid system*. Proc. IEEE Region 10 Humanitarian Technology Conference (R10-HTC), 21–23 December 2016, Agra, India, IEEE Conference Publications (2016), 1–5.

[9] Y. Yao, B. Chen, C. Tian: *Modeling and characteristics research on EHV magnetically controlled reactor*. Proc. IEEE International Power Engineering Conference (IPEC), 3–6 December 2007, Singapore, Singapore, IEEE Conference Publications (2007), 425–430.

[10] R. Bramanpalli: *Accurate calculation of AC losses of inductors in power electronic applications*. Proc. PCIM Europe 2016; International Exhibition and Conference for Power Electronics, Intelligent Motion, Renewable Energy and Energy Management, 10–12 May 2016, VDE Conference Publications (2016), 1–8.

[11] X. Wei, Y. Ji, J. Wang, G. Tan: *Orthogonal core harmonic model analysis with magnetization curve and magnetic saturation*. Proc. IEEE International Conference on Industrial Technology (ICIT), 15–17 December 2006, Mumbai, India, IEEE Conference Publications (2006), 2148–2153.

[12] B. Chen, Y. Gao, M. Nagata, K. Muramatsu: *Investigation on harmonics suppression of saturable magnetically controlled reactor using nonlinear magnetic field analysis*. Proc. IEEE International Conference on Electromagnetic Field Problems and Applications (ICEF), 19–21 June 2012, Dalian, Liaoning, China, IEEE Conference Publications (2012), 1–4.

[13] K. Nakamura, S. Hayakawa, S. Akatsuka, T. Ohinata, K. Minazawa, O. Ichinokura: *Three-dimensional reluctance network analysis considering an iron loss characteristic for an EIE-core variable inductor*. IEEE Transactions on Magnetics *41* (2005), No. 10, 4033–4035.

[14] A. Lamecki, L. Balewski, M. Mrozowski: *Effect of mesh deformation on the accuracy of 3D FEM electromagnetic analysis*. Proc. IEEE MTT-S International Conference on Numerical Electromagnetic and Multiphysics Modeling and Optimization (NEMO), 27–29 July 2016, Beijing, China, IEEE Conference Publications (2016), 1–2.

Received May 7, 2017